Monthly Notices
of the
ROYAL ASTRONOMICAL SOCIETY

Mon. Not. R. Astron. Soc. **416,** 1077–1091 (2011) doi:10.1111/j.1365-2966.2011.19104.x

Three new bricks in the wall: Berkeley 23, Berkeley 31 and King 8⋆

Michele Cignoni,[1,2]† Giacomo Beccari,[3] Angela Bragaglia[2] and Monica Tosi[2]

[1]*Dipartimento di Astronomia, Università di Bologna, via Ranzani 1, 40127 Bologna, Italy*
[2]*INAF-Osservatorio Astronomico di Bologna, via Ranzani 1, 40127 Bologna, Italy*
[3]*European Southern Observatory, Karl Schwarzschild Str 2, D-85748 Garching bei München, Germany*

Accepted 2011 May 19. Received 2011 May 13; in original form 2011 March 31

ABSTRACT

A comprehensive census of Galactic open cluster properties places unique constraints on the Galactic disc structure and evolution. In this framework, we investigate the evolutionary status of three poorly studied open clusters, Berkeley 31, Berkeley 23 and King 8, all located in the Galactic anticentre direction. To this aim, we make use of deep Large Binocular Telescope observations, reaching more than 6 mag below the main-sequence turn-off. To determine the cluster parameters, namely age, metallicity, distance, reddening and binary fraction, we compare the observational colour–magnitude diagrams (CMDs) with a library of synthetic CMDs generated with different evolutionary sets (Padova, FRANEC and FST) and metallicities. We find that Berkeley 31 is relatively old, with an age between 2.3 and 2.9 Gyr, and rather high above the Galactic plane, at about 700 pc. Berkeley 23 and King 8 are younger, with best-fitting ages in the range 1.1–1.3 and 0.8–1.3 Gyr, respectively. The position above the Galactic plane is about 500–600 pc for the former and 200 pc for the latter. Although a spectroscopic confirmation is needed, our analysis suggests a subsolar metallicity for all three clusters.

Key words: Hertzsprung-Russell and colour-magnitude diagrams – Galaxy: disc – open clusters and associations: general – open clusters and associations: individual: Berkeley 31 – open clusters and associations: individual: Berkeley 23 – open clusters and associations: individual: King 8.

1 INTRODUCTION

This paper is part of the Bologna Open Cluster Chemical Evolution (BOCCE) project, described in detail by Bragaglia & Tosi (2006) and aimed at deriving precise and homogeneous ages, distances, reddenings and chemical abundances for a large sample of open clusters (OCs). Our final goal is to study the disc of our Galaxy and its formation and evolution. In fact, OCs are among the best tracers of the disc properties (e.g. Panagia & Tosi 1981; Friel 1995; Twarog, Ashman & Anthony-Twarog 1997; Freeman & Bland-Hawthorn 2002). We have already published results based on photometry for 23 OCs (see Bragaglia & Tosi 2006; Andreuzzi et al. 2011, and references therein), concentrating on the old ones, the most important to study the early epochs of the Galactic disc. With the three OCs presented here we have a sample of 20 clusters with ages older than 1 Gyr, i.e. about 10 per cent of all known old clusters (see the catalogue by Dias et al. 2002b and its web updates).

The three clusters examined in this paper are Berkeley 23 ($l = 192.^{\circ}6$, $b = 5.^{\circ}4$), Berkeley 31 ($l = 206.^{\circ}2, b = 5.^{\circ}1$) and King 8 ($l = 176.^{\circ}4, b = 3.^{\circ}1$). They are old, distant clusters in the anticentre direction. They were selected because they should all lie beyond a Galactocentric distance of 12 kpc and could then be useful to understand the nature and properties of the outer Galactic disc. In particular, they are located in the region where the radial metallicity distribution seems to change its slope (e.g. Friel, Jacobson & Pilachowski 2010; see the discussion in Andreuzzi et al. 2011).

These three clusters have already been studied to different degrees in the past, but with contrasting results. We present here high-quality photometric data to improve on the previous determinations of their parameters. As done for all our past work, we use the comparison of observational CMDs to synthetic ones generated using different sets of evolutionary tracks.

⋆Based on observations collected at the Large Binocular Telescope (LBT) and in part at the Italian Telescopio Nazionale Galileo (TNG). The LBT is an international collaboration among institutions in the United States, Italy and Germany. LBT Corporation partners are: The University of Arizona on behalf of the Arizona University system; Istituto Nazionale di Astrofisica, Italy; LBT Beteiligungsgesellschaft, Germany, representing the Max-Planck Society, the Astrophysical Institute Potsdam, and Heidelberg University; The Ohio State University, and The Research Corporation, on behalf of The University of Notre Dame, University of Minnesota and University of Virginia. The TNG is operated on the island of La Palma by the Fundación Galileo Galilei of the INAF (Istituto Nazionale di Astrofisica) at the Spanish Observatorio del Roque de los Muchachos of the Instituto de Astrofisica de Canarias.

†E-mail: michele.cignoni@unibo.it

© 2011 The Authors
Monthly Notices of the Royal Astronomical Society © 2011 RAS

Downloaded from http://mnras.oxfordjournals.org/ at UniversitÃ di Pisa on October 13, 2016

Berkeley 23 has been the subject of two photometric works. Ann et al. (2002) observed it with a 1.8-m telescope in *UBVI* as part of a study of 12 OCs, deriving a reddening $E(B-V) = 0.40 \pm 0.05$ (from the two-colour diagram), a distance modulus $(m-M)_0 = 14.2 \pm 0.3$, a metallicity [Fe/H] $= +0.07$ and an age of 0.79 Gyr. However, the isochrone they chose does not seem to reproduce the red clump (RC). Hasegawa et al. (2004) observed 14 OCs with a 65-cm telescope, obtained *BVI* photometry and derived the clusters' parameters using isochrones. Their results for Be 23 differ from the previous ones: $E(B-V) = 0.30$, $(m-M)_0 = 13.81$, metallicity $Z = 0.004$ (equivalent to [Fe/H] $\simeq -0.7$) and age 1.8 Gyr. Ahumada & Lapasset (2007), who presented a catalogue of blue straggler stars in OCs (they have about 1900 candidate BSS in about 430 clusters), find that Be 23 is rich in this kind of stars.

Berkeley 31 is the best studied of the three OCs. Guetter (1993) published *UBVI* photometry obtained at the 1-m USNO telescope. He determined the reddening and the metallicity using the two-colour diagram, and the distance and age with an isochrone fit, deriving $E(B-V) = 0.13$, $(m-M)_0 = 13.6$, [Fe/H] $= -0.4$, and age of 8 Gyr. This old age is probably an artefact of the outdated stellar models. Furthermore, the isochrones shown do not reach the RC, while the difference in magnitude between it and the main-sequence (MS) turn-off (TO) is a powerful age indicator (for different definitions of δV see e.g. Twarog & Anthony-Twarog 1989; Phelps, Janes & Montgomery 1994). Phelps et al. (1994) obtained *VI* photometry, but could not directly derive δV; the value they give would put Be 31 at the same age of M67. Hasegawa et al. (2004), who call it Biurakan 7, derive $E(B-V) = 0.15$, $(m-M)_0 = 14.83$, $Z = 0.008$ and age of 2.2 Gyr from the isochrone fit. The discording results are not limited to the photometry. Friel et al. (2002), using low-resolution spectra of 24 stars (17 defined as members), derived an average radial velocity $\langle \mathrm{RV} \rangle = +41$ (rms $= 15$) km s^{-1} and a metallicity [Fe/H] $= -0.40$ (rms 0.16) dex. Yong, Carney & Teixera de Almeida (2005) obtained high-resolution spectra for five stars; they note that the RV dispersion is very high for an OC, maybe because they observed by chance a large fraction of binaries or because their sample includes field stars with RV similar to that of Be 31. They were able to perform an abundance analysis only on one star and derived [Fe/H] $= -0.57$. A similar situation was found by Friel et al. (2010), who obtained high-resolution spectra of another two stars, with discrepant RVs – differing also from the values by Yong et al. (2005) – and metallicity (although the two values [Fe/H] $= -0.22$ and -0.32 are not too distant). They could not determine which of the two stars, if any, is a true cluster member. They also noted that the published proper motions (Dias, Lépine & Alessi 2002a) should be of field stars in the direction of the cluster, given their bright magnitudes. Finally, also for Be 31, Ahumada & Lapasset (2007) found a large number of BSS.

The first photometry (in the *GRU* filters) of King 8 was published by Svolopoulos (1965), who described a young cluster with an age of about 5 Myr, $E(B-V) = 0.34$ and $(m-M)_0 = 13.3$. Christian (1981) presented *BV* photographic photometry and low-resolution spectra. She gave $E(B-V) \simeq 0.7$ (with a possible differential reddening up to 0.1 mag), $Z < 0.001$, distance from the Sun of 3–4 kpc and age of 0.8 Gyr. These values were partially changed by Christian (1984), where $E(B-V) = 0.55$ and [Fe/H] $\simeq -0.4$ or -0.5 dex. These two works were later used by Twarog et al. (1997) to derive a larger distance, $(m-M) = 15.30$, adopting the metallicity [Fe/H] $= -0.46$ of Friel & Janes (1993), based on two stars observed at low resolution. Koposov, Glushkova & Zolotukhin (2008) re-discovered King 8 in their automated search for new OCs on the Two micron All Sky Survey (2MASS) images. They derived the cluster parameters using isochrones in the $J, J-H$ plane, finding $E(B-V) = 0.44$, distance from the Sun of 2.4 kpc and age of 1.1 Gyr. They also noted that their numbers differ from what is listed in the Dias et al. (2002b) catalogue.

In summary, even if apparently these three OCs have already been studied, their properties are still insecure. Be 23 could be rather young and metal rich (Ann et al. 2002: 0.79 Gyr, [Fe/H] $= +0.07$) or rather old and metal poor (Hasegawa et al. 2004: 1.8 Gyr, [Fe/H] $= -0.7$). Be 31 could be very old or of intermediate age and at very different Galactocentric radii (Guetter 1993: 8 Gyr, 13 kpc; Hasegawa et al. 2004: 2.2 Gyr, 17 kpc), while there is some concordance on $E(B-V)$ around 0.13–0.15 and metallicity around -0.4 dex (but with caveats on membership). King 8 has probably an age around 1 Gyr and subsolar metallicity, but the reddening and distance are uncertain (Twarog et al. 1997: $E(B-V) = 0.55$, $\mathrm{d}_\odot = 5.24$ kpc; Koposov et al. 2008: $E(B-V) = 0.44$, $\mathrm{d}_\odot = 2.4$ kpc).

In this paper, we will describe our new observations and the resulting CMDs (Section 2), the radial extension of the clusters (Section 3), the derivation of their age, distance, reddening and metallicity comparing with synthetic CMDs (Section 4). A discussion and summary is presented in Section 5.

2 THE DATA

2.1 Observations

The three clusters were observed in service mode at the Large Binocular Telescope (LBT) on Mt Graham (Arizona) with the Large Binocular Camera (LBC) in 2008. There are two LBCs, one optimized for the UV–blue filters and one for the red–IR ones, mounted at each prime focus of the LBT. Each LBC uses four EEV chips (2048 × 4608 pixels) placed three in a row and the fourth rotated 90° with respect to the others. The field of view of the LBC is equivalent to 23 × 23 arcmin^2, with a pixel sampling of 0.23 arcsec. For technical reasons, only LBC-blue was available at the time of our observations, so we collected only *B* and *V* data. The clusters were positioned in the central chip (no. 2) of the LBC-blue CCD mosaic. Table 1 gives a log of the observations. While the seeing was good (below 1 arcsec for all images and below 0.8 arcsec for many), the observing conditions were not photometric. To calibrate our photometry, we obtained a few shallow images using DOLORES (Device Optimized for the LOw RESolution) at the Italian Telescopio Nazionale Galileo (TNG) on a night dedicated to another programme and to service observations. For this instrument the field of view is 8.6 × 8.6 arcmin^2, with a scale of 0.252 arcsec pixel^{-1}. The seeing was bad (about 3 arcsec), but this is not a problem since the fields are not crowded. Only the central part of the clusters was observed, barely reaching stars at the turn-off of the main sequence. The two standard star fields PG0918+029 and PG1323−085 from Landolt (1992) were also obtained.

2.2 Data reduction

Given the large area covered by the LBC and the small angular dimensions of our targets (see Sections 3 and 4), we only reduced two of the four chips: the one centred on the cluster (chip no. 2) and the other to be used as a comparison to separate the cluster from the field stars (chip no. 1).

The raw LBC images were corrected for the bias and flat-field, and the overscan region was trimmed using a pipeline specifically developed for LBC image pre-reduction by the Large Survey

Downloaded from http://mnras.oxfordjournals.org/ at UniversitÃ di Pisa on October 13, 2016

Table 1. Log of observations for the LBT and TNG. The exposure times are in seconds.

Cluster	RA (2000)	Dec. (2000)	Date	*B* exposure time (s)	*V* exposure time (s)
			LBC@LBT		
Be 23	06 33 15	+20 34 50	2008 December 2	1, 3 × 5, 4 × 90	1, 3 × 5, 3 × 60
Be 31	06 57 37	+08 21 18	2008 December2	1, 3 × 5, 3 × 90	1, 3 × 5, 3 × 60
King 8	05 49 24	+33 40 60	2008 December 2	1, 3 × 5, 4 × 90	1, 3 × 5, 3 × 60
			DOLORES@TNG		
Be 23	06 33 15	+20 31 30	2009 January 3	10, 20	5, 10, 20
Be 31	06 57 37	+08 17 20	2009 January 3	10, 20	10, 20
King 8	05 49 18	+33 37 50	2009 January 3	10, 20	10, 20

Table 2. Completeness of the photometry for the three clusters.

Mag	Compl *B*	Compl *V*	Compl *B*	Compl *V*	Compl *B*	Compl *V*
	Be 23		Be 31		King 8	
17.25	1.00 ± 0.11	0.99 ± 0.05	0.95 ± 0.11	0.96 ± 0.06	0.98 ± 0.05	0.99 ± 0.02
17.75	1.00 ± 0.11	0.98 ± 0.04	0.95 ± 0.12	0.97 ± 0.06	0.98 ± 0.05	0.99 ± 0.04
18.25	0.99 ± 0.06	0.98 ± 0.04	0.98 ± 0.09	0.98 ± 0.05	0.99 ± 0.04	0.99 ± 0.03
18.75	0.98 ± 0.04	0.97 ± 0.03	0.97 ± 0.06	0.97 ± 0.05	0.99 ± 0.04	0.98 ± 0.03
19.25	0.97 ± 0.04	0.97 ± 0.03	0.98 ± 0.05	0.95 ± 0.04	0.98 ± 0.03	0.97 ± 0.03
19.75	0.98 ± 0.03	0.97 ± 0.03	0.97 ± 0.05	0.96 ± 0.04	0.98 ± 0.03	0.97 ± 0.03
20.25	0.97 ± 0.03	0.96 ± 0.03	0.96 ± 0.04	0.95 ± 0.04	0.98 ± 0.03	0.97 ± 0.03
20.75	0.97 ± 0.03	0.95 ± 0.03	0.96 ± 0.04	0.94 ± 0.04	0.98 ± 0.03	0.96 ± 0.02
21.25	0.98 ± 0.03	0.94 ± 0.03	0.95 ± 0.04	0.92 ± 0.04	0.97 ± 0.03	0.95 ± 0.02
21.75	0.96 ± 0.03	0.93 ± 0.03	0.94 ± 0.04	0.90 ± 0.03	0.96 ± 0.03	0.95 ± 0.02
22.25	0.95 ± 0.03	0.90 ± 0.02	0.94 ± 0.04	0.89 ± 0.03	0.96 ± 0.02	0.92 ± 0.02
22.75	0.94 ± 0.03	0.87 ± 0.02	0.90 ± 0.03	0.84 ± 0.03	0.95 ± 0.02	0.90 ± 0.02
23.25	0.91 ± 0.02	0.78 ± 0.02	0.88 ± 0.03	0.80 ± 0.03	0.93 ± 0.02	0.88 ± 0.02
23.75	0.89 ± 0.02	0.55 ± 0.02	0.85 ± 0.03	0.72 ± 0.02	0.93 ± 0.02	0.80 ± 0.02
24.25	0.85 ± 0.02	0.29 ± 0.01	0.82 ± 0.03	0.53 ± 0.02	0.89 ± 0.02	0.59 ± 0.01
24.75	0.74 ± 0.02	0.10 ± 0.01	0.73 ± 0.02	0.26 ± 0.01	0.83 ± 0.02	0.26 ± 0.01

Center team at the Rome Astronomical Observatory.[1] The source detection and relative photometry were performed independently on each *B* and *V* image, using the point spread function-fitting code DAOPHOTII/ALLSTAR (Stetson 1987, 1994). The brightest stars, saturated in the deepest images, were efficiently recovered through the accurate magnitude measures from the short exposure time images. The average and the standard errors of the mean of the independent measures obtained from the different images were adopted as the final values of the instrumental magnitude and uncertainty.

More than 300 stars from the *Guide Star Catalogue 2.3* were used as astrometric standards to find an accurate astrometric solution to transform the instrumental positions, in pixels, into J2000 celestial coordinates. To this aim, we adopted the code CATAXCORR, developed by Paolo Montegriffo at INAF, Osservatorio Astronomico di Bologna, and successfully used by our group in the past 10 years. The rms scatter of the solution was ∼0.3 arcsec in both right ascension (RA) and declination (Dec.).

We derived the completeness level of the photometry by means of extensive artificial stars experiments following the recipe described in Bellazzini et al. (2002). More than 150 000 artificial stars have been uniformly distributed on the chip sampling the cluster in groups of 9000 stars at a time to avoid changing the crowding conditions. The whole data reduction process has been repeated as in the real case, and the fraction of recovered stars was estimated at each magnitude level. We also checked that the completeness does not change from the central to the external parts. Results for the three clusters are presented in Table 2.

With the standard stars observed at the TNG we derived the following calibration equations:

$$B = b + 0.1024 \times (b - v) + 1.3580 \ (\mathrm{rms} = 0.0118)$$

$$V = v - 0.0506 \times (b - v) + 1.0416 \ (\mathrm{rms} = 0.0167),$$

where B and V are the calibrated magnitudes and b and v are the instrumental ones (after aperture correction). Finally, the deep LBT catalogues were cross-correlated with the calibrated, shallow TNG ones and the stars in common were used as 'secondary standards' to extend the calibration to the whole catalogues, both for the central and the external chips.

We produced three catalogues with identification, equatorial coordinates, *B* and *V* magnitudes, with errors containing about 3600, 6500 and 4000 stars for Be 23, Be 31 and King 8, respectively. These catalogues will be made public through the WEBDA[2].

Fig. 1 shows the resulting CMDs from our photometry for the central and comparison field chips (upper and lower panels, respectively). In the upper panels, we also indicate the photometric errors in magnitude and colour as derived from extensive artificial star tests. They range from less than 0.01 mag at the bright limit to less than 0.1 mag around $V = 24$. The three OCs are visible over the field background, but they represent a minority of the stars in each

[1] http://lsc.oa-roma.inaf.it/

[2] http://www.univie.ac.at/webda/webda.html

Downloaded from http://mnras.oxfordjournals.org/ at UniversitÃ di Pisa on October 13, 2016

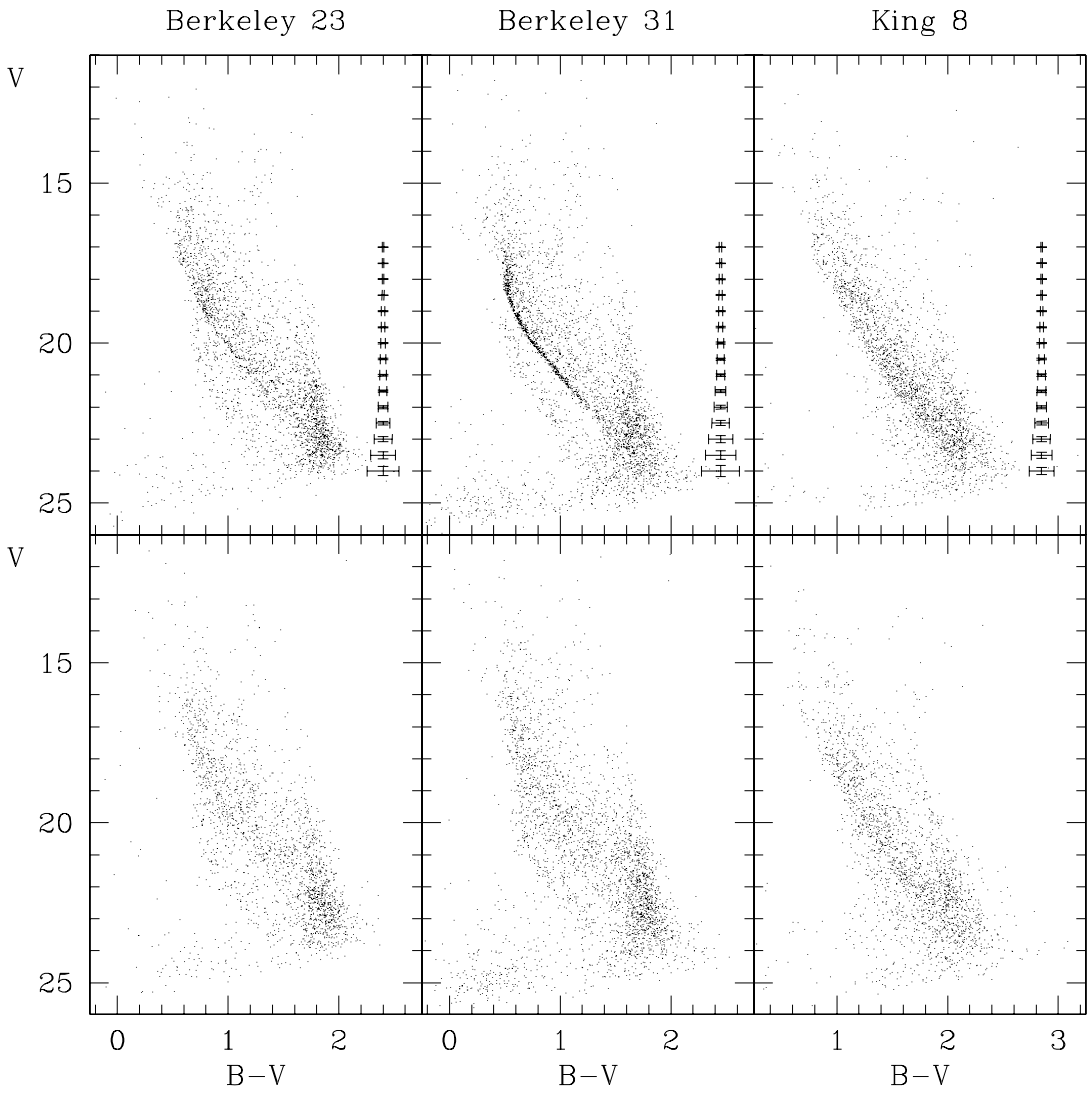

Figure 1. Upper panels: CMDs of Be 23, Be 31 and King 8 (chip no. 2). Lower panels: CMDs of the relative comparison fields (chip no. 1). Photometric errors, as derived from the artificial star tests, are shown on the right-hand side of the CMDs.

frame. In the most favourable case, Be 31, the MS is rather tight and clearly extended down to $V \approx 23$–24, while for Be 23 and King 8 the MS is recognizable from the field with some difficulty. A discussion of the field population sampled in these CMDs is presented in Section 5.

2.3 Comparison to previous data

We compare our photometry for the three OCs with Ann et al. (2002) for Be 23, Guetter (1993) for Be 31 and Christian (1981) for King 8. We do not consider the photometry of Be 31 by Phelps et al. (1994) because it has only V and I and that of Hasegawa et al. (2004) of Be 31 and Be 23 because they made public through the WEBDA only the bright stars ($V \leq 18$).

We downloaded the literature photometry files from the WEBDA site and cross-correlated our catalogues with them. Figs 2–4 show the results of the comparison between our and literature magnitudes.

For Be 23 (Fig. 2), the difference in the B filter is very small (on average -0.013 mag), while the V shows a small trend with magnitude. We do not know if this is due to our photometry or theirs; however, no trend is present for the two other OCs that were

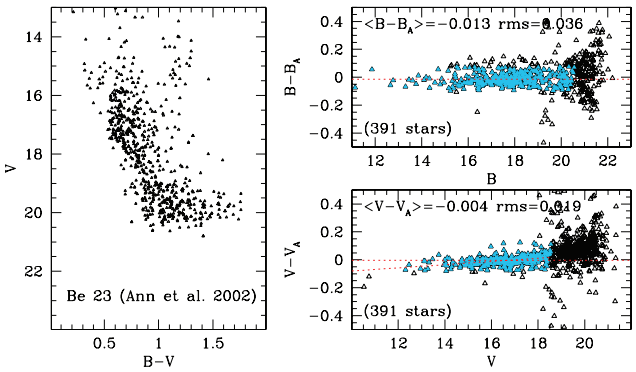

Figure 2. CMD of Be 23 by Ann et al. (2002) on the same scale used for next figures with our data. Right-hand panels: differences between our magnitudes and theirs, in B (upper panel) and V (lower panel). Open symbols indicate all stars in common and light-blue-filled symbols indicate the stars within 2σ from the average, used to compute the mean differences.

Downloaded from http://mnras.oxfordjournals.org/ at UniversitÃ di Pisa on October 13, 2016

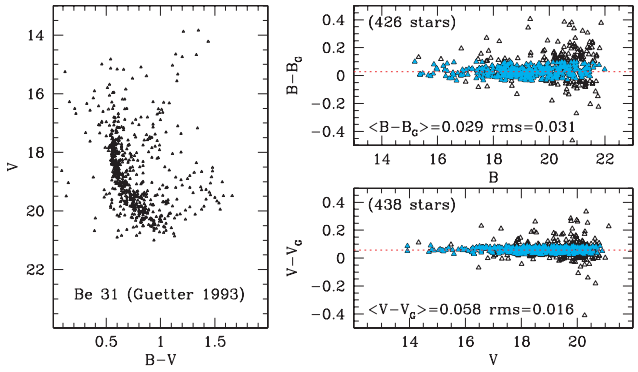

Figure 3. Left-hand panel: CMD of Be 31 by Guetter (1993) and comparison with our data (see the previous figure).

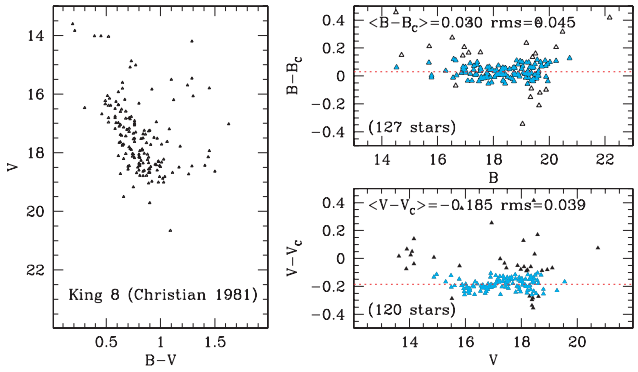

Figure 4. Left-hand panel: CMD of King 8 by Christian (1981) and comparison with our data (see the previous figures).

calibrated with the same equations, and this is in favour of the latter possibility. In the same figure, we also show the CMD obtained by Ann et al. (2002) to give an immediate impression of the much better quality of our data (see Fig. 1).

In the case of Be 31 (Fig. 3), we find small average differences both in B and V (0.029 and 0.058 mag, respectively), and no trends. The CMD by Guetter (1993), even if of good quality, is poorer than ours, which reaches fainter and shows details (e.g. near the MS TO) not visible in Guetter's CMD.

Finally, King 8 (Fig. 4) has only the photographic data by Christian (1981). While the difference between the two B values is small (-0.030 mag), for V we reach an average -0.185 mag. Again, this cluster was calibrated exactly as the other two and, given the much smaller differences with completely independent sources found for the other OCs, we think that the problem is (mostly) in the old photographic photometry.

3 THE RADIAL PROFILES

Taking advantage of the combination of the wide field and deep imaging capabilities of the LBC on the LBT, we determined the cluster structural parameters from the star's density profiles. As a first step, the centre of gravity ($C_{\rm grav}$) was estimated simply by averaging the α and δ coordinates of cluster stars. In order to avoid completeness effects and strong field contamination, we considered samples with different limiting magnitudes ($V < 20, 20.5, 21$) and with colour $B - V < 1.5$. For each sample, we iteratively calculated the barycentre of the stars (see Beccari et al. 2006) inside a circular area of 70 arcsec radius. The size of the area, somehow arbitrary, allows us to sample a gradient in the stellar radial distribution (see details later on in this paragraph) and to minimize field contamination when not removed after colour and magnitude cuts. The centre of gravity has been calculated as the average of the measures in the three magnitude ranges and the standard deviation as the related error. The values of $C_{\rm grav}$ and relative errors are reported in Table 3, where we also indicate the coordinates found in the WEBDA, since they are slightly different.

The projected density profile was determined for each cluster using direct star counts following the procedure described in Lanzoni et al. (2010). Shortly, the photometric catalogue is divided in concentric annuli centred on the cluster $C_{\rm grav}$. Each annulus is then divided in at least three angular sectors. The density of the annulus is calculated as the mean of the stellar density in each sector with the standard deviation of the mean used as the associated error. The observed radial density profile for each target cluster is shown in Fig. 5, with the abscissas corresponding to the mid-point of each radial bin. Note that, in order to minimize field contamination, we used only stars with magnitudes $V < 21$ and colour $B - V < 1.5$.

The cluster structural parameters can be estimated through a best-fitting procedure of the derived density profile with a suitable King (1966) model (as done e.g. in Sollima et al. 2010). An isotropic, single-mass King model projected on to the cluster area was computed adopting the Sigurdsson & Phinney (1995) code. The model producing the best fit for each cluster is shown in Fig. 5, together with the structural parameters core radius ($r_{\rm c}$), half-mass radius ($r_{\rm h}$), tidal radius ($r_{\rm t}$) and concentration ($c = \ln(r_{\rm t}/r_{\rm c})$, all indicated in Table 3. The residual of the fit of the model with each observed point is shown in the lower panel of each density plot. Note that the estimate of the background level is based on the star counts in the peripheral regions where the number of field stars is significantly higher than that of cluster stars.

4 CLUSTERS' PARAMETERS VIA SYNTHETIC COLOUR–MAGNITUDE DIAGRAMS

In order to determine age, metallicity, distance, mean Galactic reddening and binary fraction, we have compared the observational CMD with a library of artificial populations Monte Carlo generated (see Tosi, Bragaglia & Cignoni 2007). Different sets of stellar tracks[3] have been applied, fitting both primary age-sensitive descriptors, such as the luminosity of the MS reddest point ('red hook', RH), the RC and the MS termination point (MSTP, evaluated at the maximum luminosity reached after the overall contraction, OvC, and before the runaway to the red) and secondary CMD features (sensitive to a broad range of parameters) such as the RH colour, the luminosity at the base of the red giant branch (RGB), the RGB colour and inclination and the RC colour. The most valuable age indicator is, in principle, the TO point, evaluated at the bluest point after the overall contraction; however, for young and intermediate-age clusters this phase is poorly populated. More in general, colour constraints are less reliable than luminosity constraints, since the former are much more influenced by theoretical uncertainties like colour transformations and the super-adiabatic convection.

[3] The same used in our past works to maintain homogeneity: the old Padova (Bressan et al. 1993; Fagotto et al. 1994), the Frascati Raphson Newton Evolutionary Code (FRANEC) (Dominguez et al. 1999) and the Full Spectrum Turbulence (FST) ones (Ventura et al. 1998). See Bragaglia & Tosi (2006) for a description of their main properties and a detailed justification of their use even if newer tracks have appeared in the meantime.

Downloaded from http://mnras.oxfordjournals.org/ at UniversitÃ di Pisa on October 13, 2016

Table 3. New clusters' structural parameters; numbers in parentheses are the errors on RA and Dec.

Cluster	RA	Dec.	RA	Dec.	r_c	r_h	r_t	c
	This paper		WEBDA					
Be 23	06 33 15 (1.24 arcsec)	20 31 57 (1.98 arcsec)	06 33 30	20 33 00	55 arcsec	178 arcsec	1458 arcsec	1.4
Be 31	06 57 37 (2.84 arcsec)	08 18 20 (2.91 arcsec)	06 57 36	08 16 00	50 arcsec	171 arcsec	1540 arcsec	1.5
King 8	05 49 18 (3.21 arcsec)	33 37 50 (2.22 arcsec)	05 49 24	33 38 00	60 arcses	89 arcsec	325 arcsec	0.7

In order to make a meaningful comparison, all synthetic CMDs are combined with stars picked from an equal area of the adjacent field which is located about 9 arcmin away from the cluster centre. For each cluster, the synthetic CMD is populated until the total number of stars (synthetic plus field) equals the observed number of cluster stars brighter than $V = 20$ and corrected for photometric errors and incompleteness, as derived from the artificial star tests.

As a first step, we seek cluster's parameters that are common to all solutions. Differential reddening and fraction of binaries are the typical cases because they are almost independent of the specific set of stellar tracks. When these quantities are fixed (essentially matching the MS width), the magnitude difference between RH, MSTP and RC is effectively used to constrain the age (see e.g. fig. 8 in Castellani et al. 2003). Once the best-fitting age is established, all remaining parameters (mean Galactic reddening, metallicity and distance) are varied till the colour of the MS and the magnitudes of RH, MSTP and RC are matched. A final test of the fit quality considers the RH, RGB and RC colours as well as the luminosity at the base of the RGB.

Critical points of this process are the MS and the RC fitting. The former issue involves the upper and the lower ends of the MS. The RH morphology can vary from a vertical orientation to a very hooked morphology with the change of age, metallicity, overshooting, microscopic physics, etc., while the inclination of the lower MS follows the equation of state and the adopted colour transformations. In this context, a combination of parameters is defined 'acceptable' when the corresponding synthetic CMD fits the 'most' of the visible MS shape. On the other hand, the RC fitting can be hampered by both theoretical and statistical uncertainties. The RC morphology and luminosity strongly depend on fundamental parameters such as the metallicity, the age and the helium content, as well as by more subtle physical inputs like the efficiency of core overshooting and the amount of mass-loss in the pre-He-burning phase (see Castellani et al. 2000 for an in-depth discussion). Moreover, the number of RC stars is rather small in all three clusters, increasing the probability of confusion with RGB and field stars and not allowing very precise constraints on the derived age.

In the following, we present the three clusters from the oldest to the youngest one. Note that we did not make use of the existing information on RVs for Be 31 because they are inconclusive regarding the membership (see Section 1 and the discussion in Friel et al. 2010) and for Be 23 because they are limited to two stars.

4.1 Berkeley 31

In this group of OCs, Be 31 is the richest in terms of members. The contamination of field stars is evident, especially above the subgiant branch and blueward of the RGB. In order to reduce the number of field interlopers, but still retain a significant number of cluster members, we restrict our sample to the stars within a radius of 2.5 arcmin from the cluster centre (that is 2.5 times r_c, slightly more than r_h, and well within r_t, see Fig. 5 and Table 3). The corresponding CMD is used for the determination of the cluster parameters. The most important features are emphasized in the left-hand panel of Fig. 6 (while the right-hand panel shows the control field CMD). First of all, the OvC gap (between $V = 17.45$ and 17.6) and the base of the RGB (around $V = 17.65$) are clearly visible. The region of the RC is not well populated, but it is at least identifiable with the mild, but in our view significant, excess[4] of stars in the magnitude range $15 < V < 15.6$ and colour $B - V \approx 1.1$–1.2.

Finally, an excess of stars running parallel and redward to the MS indicates that a fraction of stars is in binary systems.

A remarkable number of stars is located blueward ($B - V < 0.4$) and mainly above ($15 < V < 17.5$) the MSTP (see Fig. 6), which cannot be explained by field stars (the control field does not contain any such blue object). As already suggested by Ahumada & Lapasset (2007), these objects are likely to be blue stragglers.

As already found several times in the past, the MS is broader than we would have expected from the photometric errors; what is surprising is that such an effect is larger around the RH. This might be a result of the combined effect of differential reddening and RH morphology. On a more speculative side, keeping in mind the strong dependence on the age of the RH morphology, it is also conceivable that the RH colour width might represent a signature of a prolonged star formation.

To solve the problem of the MS scatter, one has to conclude that either a differential reddening of about $E(B - V) = 0.05$ is present or a large fraction of binaries hosts very low-mass companions (the photometric properties of a binary system are very close to the one of the primaries alone, if the primary is below 2 $M_\odot$ and the companion's mass is less than half the primary's mass; see e.g. fig. 1 in Hurley & Tout 1998) or both. Given the patchy nature of the obscuring material in the Galactic thin disc, we are more inclined to the reddening hypothesis. In addition to the mean Galactic reddening, in the following we will adopt a differential reddening[5] of about 0.05 mag, unless otherwise stated.

A rough estimate of the binary fraction can be obtained by evaluating the number of stars in two appropriate CMD boxes: one along the MS (see the dotted line in Fig. 6) and one redward of the MS (chosen to cover the binary sequence; see the dot-dashed line). We apply magnitude cuts and keep only stars below the RH and brighter than $V = 22$ to avoid evolved stars where the binary evolution can be quite complicated. To remove the field contamination, we have statistically subtracted the contribution of field stars using several equal area regions randomly chosen from the control field. The net result is a binary fraction between 22 and 26 per cent. Strictly speaking, these estimates may be slightly underestimated with respect to the real fraction, since low mass ratio binaries, whose properties are

[4] Such an excess is found with respect to other equal-area CMD, randomly chosen from the control field.

[5] Here, the total reddening is considered as a sum of a mean Galactic component and a random component (differential) which includes the foreground fluctuation and a possible internal reddening.

Downloaded from http://mnras.oxfordjournals.org/ at UniversitÃ di Pisa on October 13, 2016

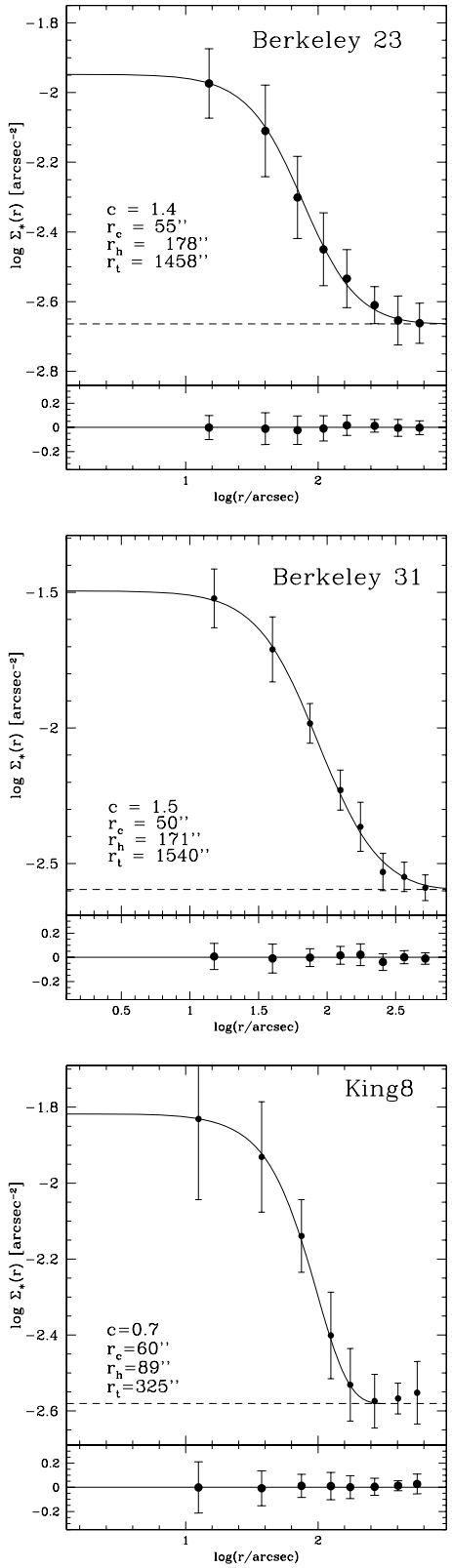

Figure 5. Observed surface density profiles (filled circles and error bars) in units of the number of stars arcsec^{-2}. The solid lines are the King models that best fit the observed density profile over the entire cluster extension.

close to those of single stars, might be partially missed. However, a mean fraction of 24 per cent appears to be a reasonable 'ansatz' and will be assumed for all the simulations.

Keeping the binary fraction and the differential reddening fixed, we have searched the best combination of parameters for each set of tracks and metallicity. Table 4 summarizes the results and the residual discrepancies. Synthetic RGB, RC and lower MS colours together with the magnitude of the RGB base are labelled as 'TB', 'TR', 'TF' or 'OK' when they are too blue, too red, too faint or in agreement with respect to the data, respectively.

Concerning the age, the overall interval of confidence is between 2.3 and 2.9 Gyr. As expected, to reproduce the observed colours, models of progressively lower metallicity require a larger mean reddening and a larger distance modulus, because they are intrinsically bluer and brighter. However, the quality of the fit subtly depends on the adopted metallicity.

The FST models with $Z = 0.006$ and 0.01 fit reasonable well the RH, MSTP and RC luminosity levels, the colour of the RGB and the magnitude of the RGB base, but they predict a 'too hooked' RH (that does not mean that the colour is wrong, but rather that the MS shape is too curved before the RH point), a synthetic MS (below the 19th magnitude) and an RC bluer than actually observed. In terms of cluster parameters, the former metallicity would suggest a cluster age of 2.6 Gyr, $E(B-V) = 0.165 \pm 0.025$ and a distance modulus $(m-M)_0 = 14.6$, the latter a cluster age of 2.8 Gyr, $E(B-V) = 0.095 \pm 0.025$ and a distance modulus $(m-M)_0 = 14.6$. Raising the metallicity to $Z = 0.02$ significantly worsens the quality of the fit. In fact, the magnitude difference between RC and MSTP requires an age of 2.7 Gyr, and any attempt to reconcile the predicted and observed RH colour and magnitude runs into two additional problems: the reddening should be lowered to an untenable $E(B-V) \approx 0.02$ (compared to the Schlegel, Finkbeiner & Davis 1998 estimate of 0.145) and the synthetic RGB would be too red.

With the Padova stellar tracks, we find that the lower metallicity, $Z = 0.004$, provides the best match, although suffering from the same pathologies noted with the $Z = 0.006$ FST set, i.e. too blue synthetic RC and the lowest MS. In this case, the estimated age raises to 2.9 Gyr, and we find a mean reddening $E(B-V) = 0.185 \pm 0.025$ and a distance modulus $(m-M)_0 = 14.4$. The metallicity $Z = 0.008$ does not improve the fit and makes the match worse, producing a too red RGB. Accepting these discrepancies we get an estimated age of 2.6 Gyr, $E(B-V) = 0.135 \pm 0.025$ and a distance modulus $(m-M)_0 = 14.45$. Finally, the Padova $Z = 0.02$ set is not acceptable for the same reason as the solar FST: matching the MSTP, RC and the RH magnitudes would require a null reddening, contrary to the Schlegel et al. (1998) values.

The FRANEC models are the only ones able to reproduce well the faint end of the MS (down to $V \approx 20-20.5$). Using the metallicity $Z = 0.006$, we can reproduce all important features apart for a mismatch in the colour of the RC that is too blue. In this case, the best combination of parameters is: the cluster age of 2.5 Gyr, $E(B-V) = 0.175 \pm 0.025$ and a distance modulus $(m-M)_0 = 14.46$. The metallicity $Z = 0.01$ reduces the RC colour discrepancy, but to the cost of a synthetic RGB that is too red by as much as ~ 0.1 mag and underluminous at the base by as much as ~ 0.25. Using $Z = 0.01$ the best set of parameters is: the age of 2.3 Gyr, $E(B-V) = 0.145 \pm 0.025$ and a distance modulus $(m-M)_0 = 14.6$. A very similar result can be achieved by using a metallicity $Z = 0.02$, provided that all the main parameters be readjusted: the age of 2.5 Gyr, differential reddening $E(B-V) = 0.025 \pm 0.025$ and a distance modulus $(m-M)_0 = 14.8$.

Downloaded from http://mnras.oxfordjournals.org/ at UniversitÃ di Pisa on October 13, 2016

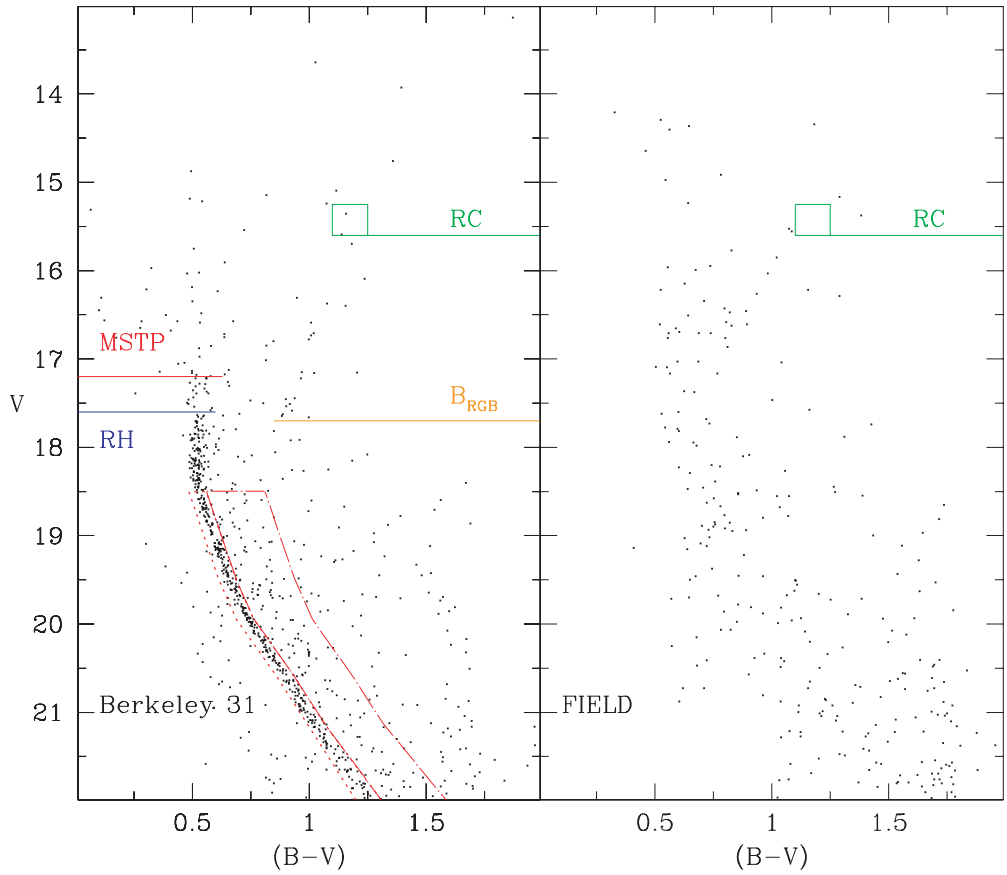

Figure 6. Left-hand panel: CMD of stars within 2.5 arcmin of the centre of Be 31. We indicate the luminosity level of the RH, the MSTP and the RC and the base of the RGB (BRGB). The dotted and the dot–dashed boxes are, respectively, used to estimate the fraction of single and binary stars. Right-hand panel: CMD of field stars (as evaluated from an equal area adjacent region).

Table 4. Be 31 best-fitting parameters (age, mean Galactic reddening, differential reddening and distance modulus) for various sets of models and metallicities. Columns from 7 to 10 indicate how the models reproduce the following CMD features: RGB colour, magnitude at the base of the RGB, RC colour, and lower MS colour. Additionally, the 10th column reports the magnitude below which the synthetic MS diverges from the data MS. See the text for the definition of the flags TR, TB, TF and OK.

Set	Z	Age (Gyr)	$E(B-V)_M$	$E(B-V)_D$	$(m-M)_0$	RGB (C)	RGB base (M)	RC (C)	Low MS (C)
FST ($\eta = 0.2$)	0.02	2.7	0.020	±0.00	14.90	TR	OK	TB	TB($V > 19$)
FST ($\eta = 0.2$)	0.01	2.8	0.095	±0.025	14.60	OK	OK	TB	TB($V > 19$)
FST ($\eta = 0.2$)	0.006	2.6	0.165	±0.025	14.60	OK	OK	TB	TB($V > 19$)
Padova	0.02	2.8	0.00	±0.00	14.75	TR	TF	OK	TB($V > 20.5$)
Padova	0.008	2.6	0.135	±0.025	14.45	TR	OK	TB	TB($V > 20.5$)
Padova	0.004	2.9	0.185	±0.025	14.40	OK	OK	TB	TB($V > 20.5$)
FRANEC	0.02	2.5	0.025	±0.025	14.80	TB	TF	TR	OK($V > 21$)
FRANEC	0.01	2.3	0.145	±0.025	14.60	TR	OK	OK	OK($V > 21$)
FRANEC	0.006	2.5	0.175	±0.025	14.46	OK	OK	TB	OK($V > 21$)

Fig. 7 summarizes the best-fitting CMD for each set of tracks, compared with the observational CMD (top-left panel).

Trying to understand the results in terms of different prescriptions of the input physics, a first interesting conclusion concerns the efficiency of the core overshooting. As expected, the RH length is severely affected by this macroscopic effect as a consequence of the longer core hydrogen burning. Models with overshooting predict ages higher (2.6–2.9 Gyr) than those inferred with canonical models (2.3–2.5 Gyr). Our analysis suggests that the observed RH morphology is better delineated by the non-overshoot tracks, as represented by the FRANEC models, while the Padova and FST solutions, which use different amounts of overshooting, are too hooked. On the other hand, the low MS is unaffected by overshooting, with these stars being characterized by radiative cores. In this case, the good match offered by low-mass FRANEC models reflects, rather, a combined effect of the equation of state and the atmosphere model.

On the basis of this discussion, the FRANEC set should be preferred, since it is in agreement with both the RH morphology and the low-MS location. This restricts the set of possible ages to the range from 2.3 to 2.5 Gyr. Concerning the metallicity, a solar abundance is ruled out by a clear inability to reproduce the RGB colour. This result is in reasonable agreement with what has been found in the literature, both by photometric and spectroscopic methods (see Section 1).

Downloaded from http://mnras.oxfordjournals.org/ at UniversitÃ di Pisa on October 13, 2016

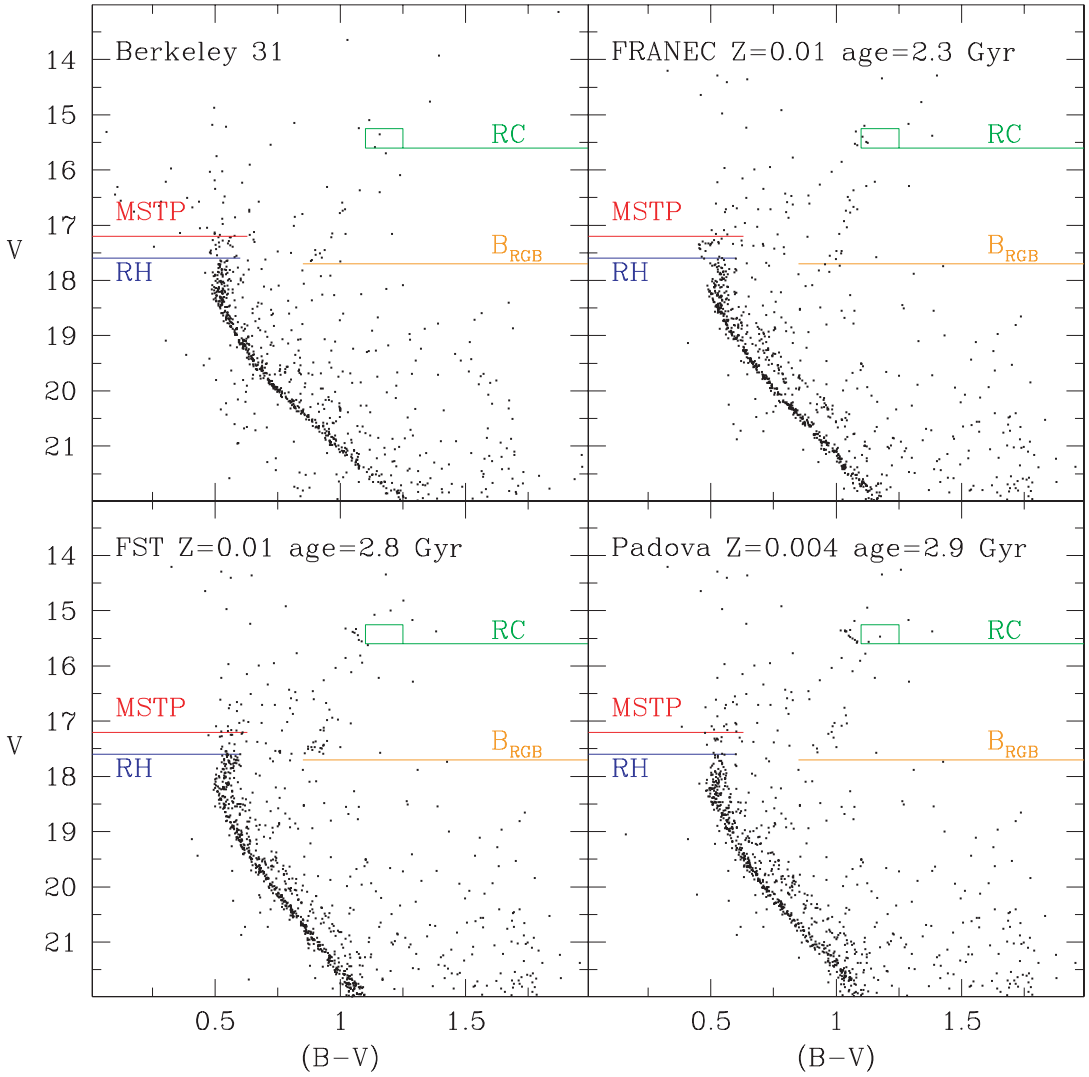

Figure 7. Top left-hand panel: CMD of stars within 2.5 arcmin of the centre of Be 31. The other panels, clockwise from this, show the best-fitting synthetic CMDs for the following parameters: FRANEC $Z = 0.01$, age 2.3 Gyr, $E(B - V) = 0.145 \pm 0.025$ and $(m - M)_0 = 14.6$; Padova $Z = 0.004$, age 2.9 Gyr, $E(B - V) = 0.185 \pm 0.025$ and $(m - M)_0 = 14.4$; FST $Z = 0.01$, age 2.8 Gyr, $E(B - V) = 0.095 \pm 0.025$ and $(m - M)_0 = 14.6$. The adopted percentage of binaries (with a random mass ratio) is always 24 per cent.

With these ranges of age and metallicity, the mean Galactic reddening is between 0.145 and 0.175 mag, only slightly higher than the Schlegel et al. (1998) estimate $E(B - V) = 0.145$ (which is an upper limit, being the asymptotic reddening in the cluster direction, but which is also more uncertain at low Galactic latitudes like those of our clusters), while the best estimate for the distance modulus is between 14.46 and 14.6.

A final comment concerns the choice of adopting a fraction of binaries of 24 per cent: surprisingly, a visual inspection of Fig. 7 seems to suggest that this number is slightly too high. However, this is clearly an artefact of the minimum mass ($0.6\,M_\odot$) in our stellar models, whose effect is to bias the binary distribution towards the high-mass ratio. Although this effect is negligible near the TO, it grows near the lower end of the MS.

4.2 Berkeley 23

The strong contamination and the apparent small number of cluster stars make the CMD of Be 23 rather poorly defined. In the left-hand panel of Fig. 8, we show the CMD restricted to the inner 3 arcmin from the cluster centre (that is about three r_c and slightly less than r_h, see Fig. 5 and Table 3). This partially cleans the diagram, revealing some signatures of the cluster: (1) a broad and irregularly clumped MS, clearly distinguishable at least down to $V = 22$, (2) an RH positioned near $V = 16.2$ (evidenced in blue), (3) an MSTP near $V = 15.7$ (in red) and (4) a mild excess of stars which is compatible with an apparently elongated RC, extending between $V = 15.1$ and 15.5 (green). The RGB, not sufficiently populated to be distinguishable from the field, is instead difficult to be recognized. This circumstance, together with the wide OvC gap and the extended RC, indicates that the cluster is younger than 2 Gyr.

Before applying the synthetic CMD approach, we have evaluated the amount of differential reddening and the fraction of binaries. The MS presents a substantial intrinsic scatter, larger than expected from photometric errors, suggesting a differential reddening of at least 0.05 mag. The percentage of binaries is not easy to obtain, given the strong field contamination. Using the same strategy applied to

Downloaded from http://mnras.oxfordjournals.org/ at UniversitÃ di Pisa on October 13, 2016

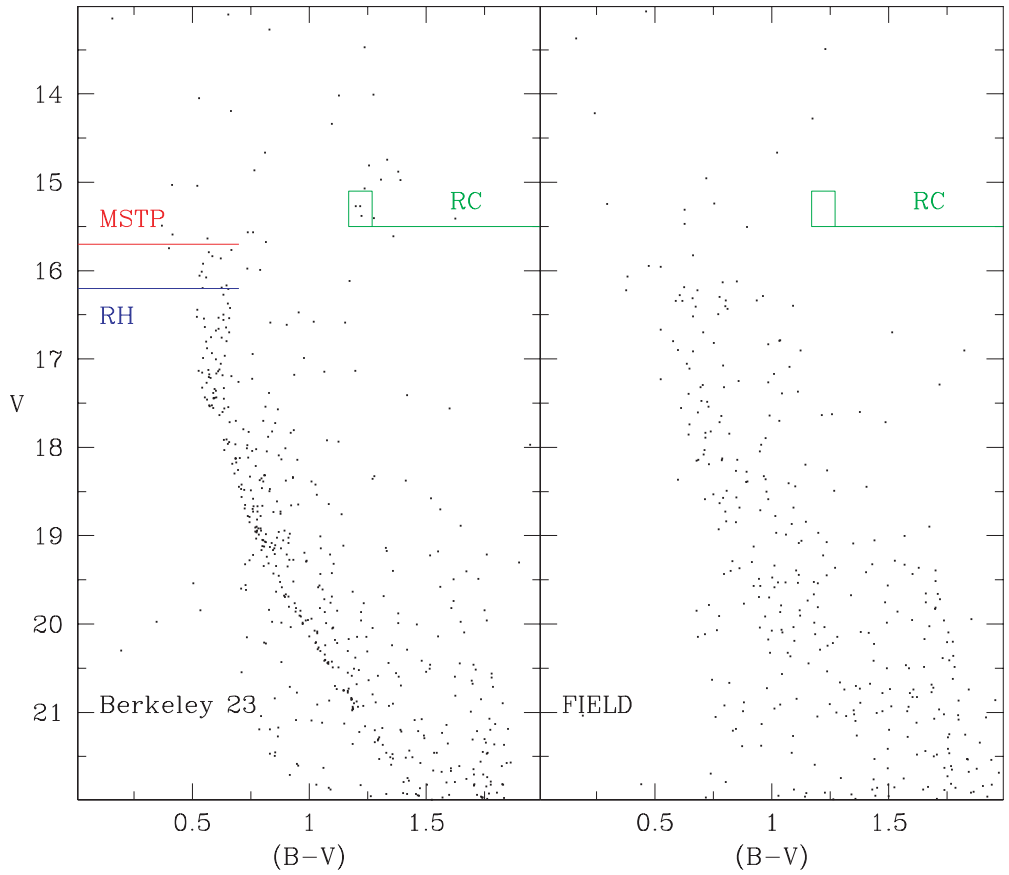

Figure 8. Left-hand panel: CMD of stars within 3 arcmin of the centre of Be 23. Labels indicate the luminosity level of the RC, the MSTP and the RH. Right-hand panel: control field CMD (taken from an equal area of the adjacent region).

Be 31, we have found a range of values between 20 and 30 per cent. Such large uncertainty should be taken as a consequence of the spatial fluctuations across the control field. In the following, we adopt a differential reddening $E(B-V) = 0.05$ and a mean fraction of binaries of 25 per cent.

In order to put limits on the cluster age and metallicity, the 3 arcmin CMD is compared with our synthetic CMDs. Generally speaking, all examined models do not satisfactorily reproduce two evident CMD features. First of all, the observed RH morphology is more vertical than predicted by the models. Furthermore, we cannot effectively reproduce the number counts at the MSTP and at the RC, which are always underpredicted by all models.

Despite these discrepancies, some conclusions can be drawn using the RH, MSTP and RC luminosities as well as the MS colour. Table 5 summarizes the best combination of parameters and the residual discrepancies for each set of tracks.

All the examined models can be reconciled with the luminosity constraints, whereas only the FST and the Padova tracks at solar metallicity can fit the average RH colour and the RC colour. In both cases the cluster age is found to be around 1.3 Gyr. At lower metallicities the synthetic RH colours become systematically too blue. This drawback is particularly severe for the FRANEC tracks. The reason for this is the younger ages required for the FRANEC set to fit the luminosity constraints (RH, MSTP and RC), since they do not consider overshooting. However, the FRANEC models work better than any other to reproduce the colour of the lower MS. In particular, these tracks are able to match the MS down to $V \approx 21$, while all other models diverge to the blue below $V \approx 20$.

Fig. 9 shows the best-fitting CMD for each set of tracks and the corresponding parameters. We have decided to give preference to the RH region, which provides information on the age, rather than the low-MS fit; hence, all FRANEC models have been rejected. With this assumption, the age for Berkeley 23 is well constrained between 1.1 and 1.3 Gyr, while the favoured metallicity is solar. Concerning reddening and distance, the range of variation for the former is 0.225–0.425 and for the latter is between 13.6 and 14.00. Furthermore, it is noteworthy that the reddening required for the solar models ($E(B-V) = 0.225 \pm 0.025$) is too low compared with the Schlegel et al. (1998) value ($E(B-V) = 0.35$), while that implied by the half-solar models is perfectly consistent, and the reddening required by even metal poorer models ($Z = 0.006$ and 0.004) is barely acceptable or too high. Combining these arguments, we suggest that the metallicity of Be 23 is probably between solar (as suggested by the CMD fitting) and half-solar.

As already noted in Section 1, there is discrepancy between different analyses of this cluster, and our study makes no exception. We disagree with Ann et al. (2002), who find the cluster to be much younger and metal richer, yet more reddened, even if these authors used MSTP and RH luminosities very close to the values adopted here (see their fig. 3). However, their best-fitting model seems to miss the RC position. We disagree also with Hasegawa et al. (2004) on the age and metallicity (their best solution is much

Downloaded from http://mnras.oxfordjournals.org/ at UniversitÃ di Pisa on October 13, 2016

Table 5. Be 23 best-fitting parameters (see previous table).

Set	Z	Age (Gyr)	$E(B-V)_M$	$E(B-V)_D$	$(m-M)_0$	RH(C)	RC (C)	Low MS (C)
FST ($\eta = 0.2$)	0.02	1.3	0.225	±0.025	14.00	OK	OK	TB ($V > 20$)
FST ($\eta = 0.2$)	0.01	1.2	0.325	±0.025	13.80	TB	OK	TB ($V > 20$)
FST ($\eta = 0.2$)	0.006	1.1	0.385	±0.025	13.75	TB	OK	TB ($V > 20$)
Padova	0.02	1.3	0.225	±0.025	14.00	OK	TR	TB ($V > 20$)
Padova	0.008	1.3	0.325	±0.025	13.75	TB	OK	TB ($V > 20$)
Padova	0.004	1.2	0.425	±0.025	13.6	TB	OK	TB ($V > 20$)
FRANEC	0.02	1.0	0.245	±0.025	13.95	TB	OK	TB ($V > 21$)
FRANEC	0.01	0.9	0.375	±0.025	13.75	TB	OK	TB ($V > 21$)
FRANEC	0.006	0.8	0.445	±0.025	13.75	TB	OK	TB ($V > 20.5$)

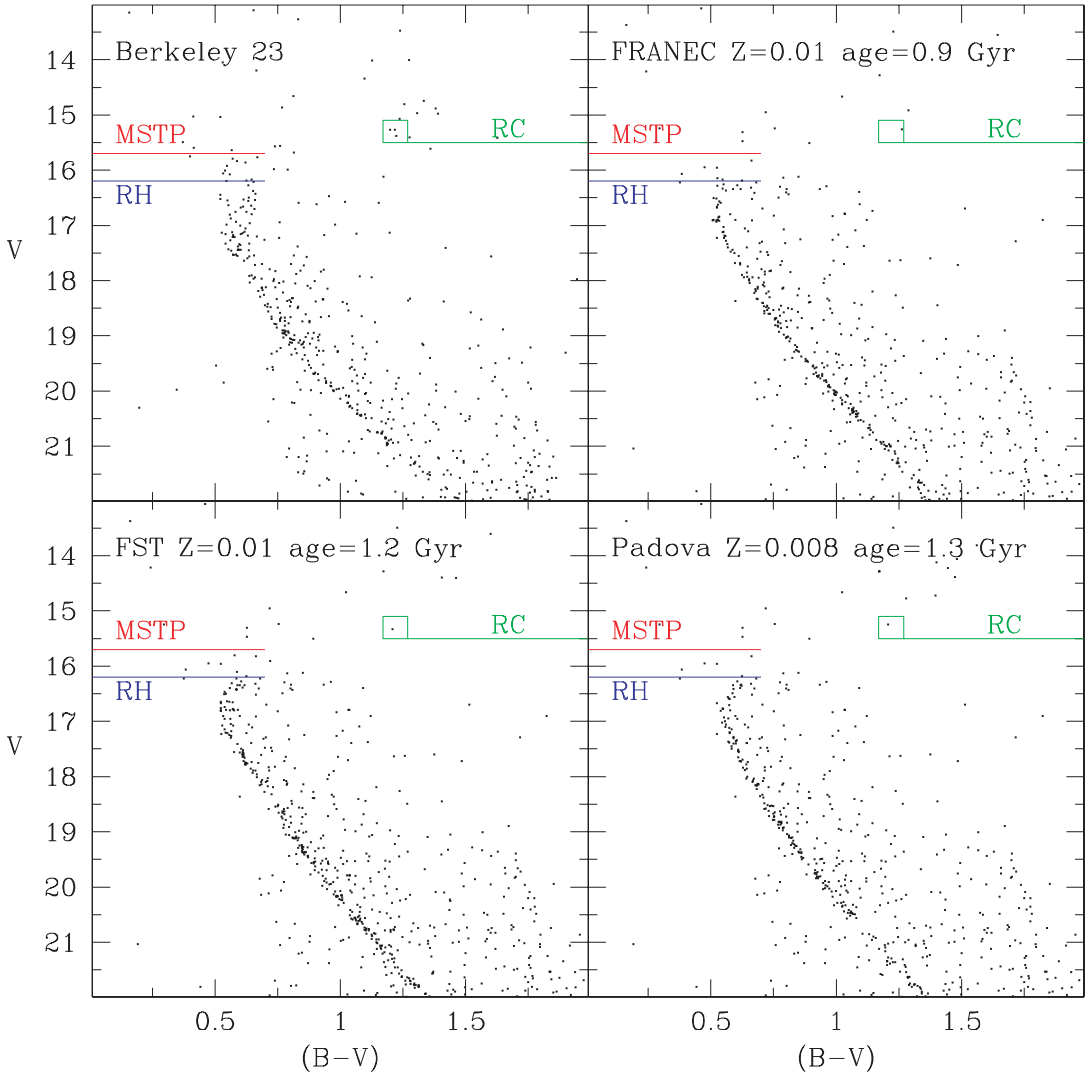

Figure 9. Top-left panel: CMD of stars within 3 arcmin of the centre of Be 23. The other panels, clockwise from this, show the best-fitting synthetic CMDs for the following parameters: FRANEC $Z = 0.01$, age 0.9 Gyr, $E(B-V) = 0.375 \pm 0.025$ and $(m-M)_0 = 13.75$; Padova $Z = 0.008$, age 1.3 Gyr, $E(B-V) = 0.325 \pm 0.025$ and $(m-M)_0 = 13.75$; FST $Z = 0.01$, age 1.2 Gyr, $E(B-V) = 0.325 \pm 0.025$ and $(m-M)_0 = 13.8$. The adopted percentage of binaries (with random mass ratio) is always 25 per cent.

older and metal poorer) even if reddening and distance modulus are in very good agreement. The age and metallicity differences arise mainly from a different interpretation of the MSTP position: by looking at their fig. 3 it is evident that these authors have identified as the MSTP a point that is half a magnitude fainter than ours.

4.3 King 8

King 8 exhibits a very scattered CMD, suggesting the strongest differential reddening among the three clusters. This is clearly evident from the left-hand panel of Fig. 10 where the CMD of stars within 3 arcmin from the cluster centre (that is, three

Downloaded from http://mnras.oxfordjournals.org/ at UniversitÃ di Pisa on October 13, 2016

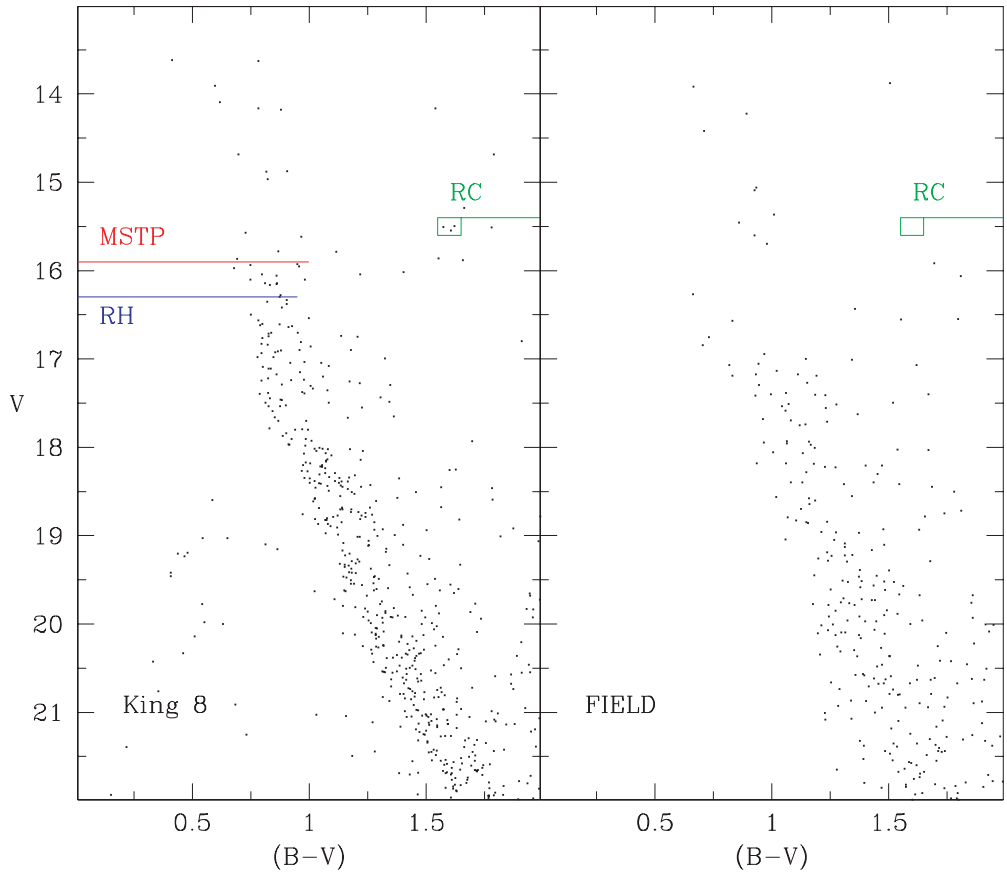

Figure 10. Left-hand panel: CMD of stars within 3 arcmin of the centre of King 8. Right-hand panel: control field CMD (as evaluated from an equal area of the adjacent region).

times r_c, $2.5r_h$ and within r_t, see Fig. 5 and Table 3) is compared with the control field CMD (right-hand panel). In these conditions, a few CMD features are available for the fit: (1) an MSTP around $V = 16.0$ (indicated with a red line in Fig. 10), (2) a wide OvC gap and (3) an RC around $V = 15.5$ (indicated with a green box). As for Be 23, there is no evidence of a well-formed RGB. More importantly, the large MS spread prevents a safe identification of the RH, which is tentatively identified as the mildly hooked feature around $V = 16.3$ (indicated with a blue line).

Given the wide (0.2 mag) and rather uniformly filled MS, the current data do not allow us to reach a firm conclusion about the binary fraction. Hence, in the following simulations, we have assumed a fixed fraction of 30 per cent (with a random mass ratio). On the other hand, a differential reddening $E(B - V)$ of at least 0.2 mag represents the only viable solution to reproduce the observed MS spread. Keeping fixed these parameters, we have investigated the possibility of fitting simultaneously the MSTP, the RH and the RC luminosities by adjusting the age, the mean Galactic reddening and the distance modulus. The best-fitting results for the various sets and metallicities are displayed in Table 6, with the last two columns describing how close the models match the RC and the lower MS colours.

In contrast with what is found for Be 23 and Be 31, all explored models match very well the lower MS (at least up to $V = 21$). On the other hand, as a consequence of the high differential reddening, all synthetic CMDs show a rather elongated RC, while the observed RC is round and concentrated. Fig. 11 summarizes the best-fitting CMD for each set of tracks compared with the data CMD (top-left panel).

With the FST models, both the solar and the half-solar metallicities fail to reproduce the RC colour (bluer than observed) and the number of stars around the MSTP phase (systematically underestimated). A much better result is achieved using the $Z = 0.006$ models, whose synthetic CMDs account for the RC colour, although still predicting too few MSTP stars. In terms of age, the $Z = 0.006$ case corresponds to about 1.1 Gyr, while the best-fitting distance is about $(m - M)_0 = 12.95$. Furthermore, the high reddening implied by the metallicity $Z = 0.006$ is in good agreement with the literature value ($E(B - V) = 0.8$) based on the Schlegel et al. (1998) maps, while the reddening solutions $E(B - V) = 0.55 \pm 0.10$ and 0.65 ± 0.10, required by the metal richer tracks, are too low or barely acceptable, respectively.

In contrast with the FST result, among the Padova models only those at solar metallicity predict the correct RC colour, whereas the synthetic RC is too blue (by about 0.1 mag) at $Z = 0.008$ and 0.004. On the other hand, no significant difference is found in the best-fitting age with varying metallicity: with $Z = 0.02$ the best CMD is for 1.3 Gyr, while with $Z = 0.004$ it is 1.1 Gyr, results which are almost identical to the FST findings. Focusing on the MSTP, both Padova and FST tracks share the same mismatch (which is to be ascribed to the overshooting): the predicted number of MSTP stars is always underestimated. As found for the FST models, the comparison with the Schlegel et al. (1998) maps reddening favours the lowest metallicity ($Z = 0.006$), in contrast with our photometric estimate.

Downloaded from http://mnras.oxfordjournals.org/ at UniversitÃ di Pisa on October 13, 2016

Table 6. King 8 best-fitting parameters. Columns 7 and 8 indicate the ability of the models to reproduce the RH colour and the lower MS colour. Additionally, the 8th column reports the magnitude below which the synthetic MS diverges.

Set	Z	Age (Gyr)	$E(B-V)_M$	$E(B-V)_D$	$(m-M)_0$	RC (C)	Low MS (C)
FST ($\eta = 0.2$)	0.02	1.2	0.55	±0.10	13.20	TB	TB ($V > 21$)
FST ($\eta = 0.2$)	0.01	1.2	0.65	±0.10	13.00	TB	TB ($V > 21$)
FST ($\eta = 0.2$)	0.006	1.1	0.75	±0.10	12.95	OK	TB ($V > 21$)
Padova	0.02	1.3	0.52	±0.10	13.20	OK	TB ($V > 21$)
Padova	0.008	1.2	0.65	±0.10	12.90	TB	TB ($V > 21$)
Padova	0.004	1.1	0.75	±0.10	12.80	TB	TB ($V > 21$)
FRANEC	0.02	0.9	0.60	±0.10	13.20	OK	TB ($V > 22$)
FRANEC	0.01	0.9	0.67	±0.10	13.00	OK	TB ($V > 22$)
FRANEC	0.006	0.8	0.78	±0.10	12.85	OK	TB ($V > 22$)

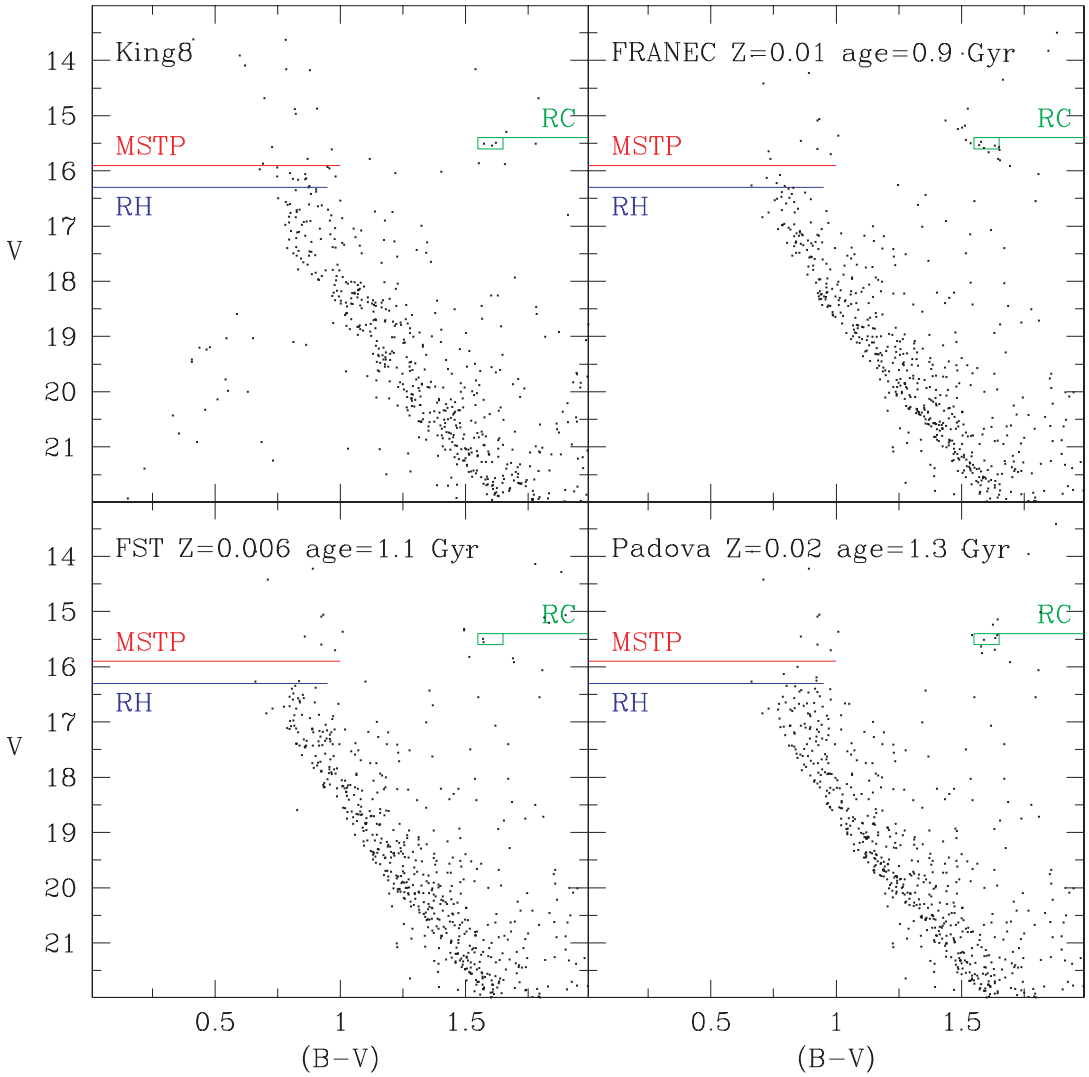

Figure 11. Top-left panel: CMD of stars within 3 arcmin of the centre of King 8. The other panels, clockwise from this, show the best-fitting synthetic CMDs for the following parameters: FRANEC $Z = 0.01$, age 0.9 Gyr, $E(B-V) = 0.67 \pm 0.10$ and $(m-M)_0 = 13.0$; Padova $Z = 0.02$, age 1.3 Gyr, $E(B-V) = 0.52 \pm 0.10$ and $(m-M)_0 = 13.2$; FST $Z = 0.006$, age 1.1 Gyr, $E(B-V) = 0.75 \pm 0.10$ and $(m-M)_0 = 12.95$. The adopted percentage of binaries (with a random mass ratio) is always 30 per cent.

As far as the FRANEC models are concerned, we do not find a clear indication to prefer one metallicity over the others. Both the observed MSTP counts and the lower MS colours are fairly well reproduced (the latter down to $V \approx 22$), while the mismatch here concerns the predicted number of RC stars (whose colours are in good agreement with the observations), which outnumber the observed counts by a factor of 3. The resulting ages (0.8–0.9 Gyr) are younger than those obtained with the Padova and FST models,

Downloaded from http://mnras.oxfordjournals.org/ at UniversitÃ di Pisa on October 13, 2016

as a direct consequence of the lack of overshooting. Once again, only the subsolar models ($Z = 0.01$ and 0.006) imply a reddening value compatible with the Schlegel et al. (1998) estimate.

Also, for this cluster the comparison to previous results is not simple. We seem to agree, apart from the Padova solution, on a rather low metal content. The apparent agreement with Christian (1981, 1984) is not significant, given the differences between the two photometries (see Fig. 4). Koposov et al. (2008) adopted solar isochrones for all their clusters and this could at least partly explain the differences, although the dependence on metallicity should be smaller in the near-IR bands.

5 CONCLUSIONS

5.1 Galactic considerations

Be 31 and Be 23 are rather far away from both the Galactic centre and the Galactic plane. Berkeley 31 has a Galactocentric distance[6] (R_{GC}) between 15.4 and 15.9 kpc and a height above the Galactic plane between 693 and 739 pc, while Berkeley 23 has an R_{GC} between 13.1 and 14.2 kpc and a height between 494 and 594 pc. Such scale heights could be the result of a formation *in situ* as a part of the thick-disc population, as also suggested by the old age of Be 31 (well over 2 Gyr) or due to a disc flaring which gradually increases the Galactic scale-height of the thin disc. On the other hand, the shorter scale height (between 196 and 236 pc), its R_{GC} between 11.6 and 12.3 kpc and the younger (probably less than 1 Gyr) age make King 8 a likely member of the thin disc.

Such findings help to interpret the difference in the field population between the direction of Be 23 and Be 31 and the direction of King 8 visible in the lower panels of Fig. 1. In the former, a structure to the blue of the clusters' MS is clearly visible starting from $V = 19$. Such a contamination is a signature of a much farther and probably older population along the line of sight. The most likely candidate is the above-mentioned thick disc (see e.g. Cignoni et al. 2008), whose scale height is at least three times longer than the corresponding thin disc. Although less probable, it may also represent a tidal debris of a disrupted galaxy (see e.g. the Monoceros ring; Martin et al. 2004) or a signature of the Galactic warp and flare (Momany et al. 2006). On the other hand, the lack of this feature in the direction of King 8 is mostly due to the closer proximity to the Galactic plane (3° against ≈5° of Be 23 and Be 31). At this latitude, the line of sight goes deeper into the thin disc (for about 6 kpc) before crossing a pure thick disc sample, making the thin disc stars the dominant contaminant. Furthermore, the Galactic reddening increases with distance; this explains the elongated shape of the M-dwarf sequence (around $B - V \sim 1.9$) exhibited by the King 8 CMD field, a circumstance that is not observed either in Be 23 or in Be 31 (where the M-dwarf sequence is rather vertical).

5.2 Summary

Our study of OCs is aimed at better understanding of the chemical and structural properties of the Galaxy. In this paper, we have studied three distant OCs towards the Galactic anticentre using deep LBT photometry. The CMDs resulting from these data are more precise and more than 3 mag deeper than the ones found in the literature, extending to more than 6 mag below the MS TOs. The synthetic CMD technique has been used to derive a confidence interval for age, metallicity, binary fraction, reddening and distance for each cluster. To remove the model dependence of the results, three different sets of stellar tracks (Padova, FST and FRANEC) have been adopted. From the comparison between models and data we have drawn the following conclusions.

(i) Be 31 is located at about 15–16 kpc from the Galactic centre and about 700 pc above the Galactic plane. The resulting age varies from 2.3 to 2.9 Gyr, depending on the adopted stellar model, with better fits for ages between 2.3 and 2.5 Gyr. Concerning the metallicity we obtained a good match using the sets of models with the metal content being lower than the solar content. The mean Galactic reddening $E(B - V)$ is between 0.095 and 0.185 mag, and the fraction of binaries is between 22 per cent and 26 per cent.

(ii) Be 23 is at about 13–14 kpc from the Galactic centre and 500–600 pc above the plane. The age is well constrained between 1.1 and 1.3 Gyr, while the best-fitting metallicity is more uncertain: the CMD fit suggests a solar value, while only a half-solar metallicity is compatible with the Schlegel et al. (1998) estimate for the Be 23's direction. The mean Galactic reddening $E(B - V)$ is between 0.225 and 0.425 and the binary fraction is between 20 per cent and 30 per cent.

(iii) King 8 is at about 12 kpc from the Galactic centre and about 200 pc above the plane. The strong differential reddening up to ±0.1 mag broadens the colour extension of the MS, hindering a precise estimate of the cluster parameters. In this condition, the best-fitting age is 0.8–1.3 Gyr, while the entire range of metallicities (0.004–0.02) is consistent with the data. On the other hand, only subsolar models lead to reddening estimates [ranging from $E(B - V) = 0.55$ to 0.88] in agreement with Schlegel et al. (1998). 30 per cent of binaries are compatible with the observed CMD.

With these results, Be 31 and Be 23 are the candidates of thick-disc OCs, while King 8 is a more classical thin-disc member. Only further direct spectroscopic and kinematic searches will allow us to shed light on the Galactic origin of these clusters. They will also be very important for any study of the radial distribution of metallicity (and chemical abundances) in the Galactic disc, a crucial ingredient in chemical evolution models.

Our choice to exploit the RC position even if it is barely visible in the three clusters deserves a final comment. For Be 31, which shows the least defined RC, many other relevant and well-defined CMD features (RH, MSTP, RGB and sharp MS) are available. Hence, even without using the RC we would get the same parameter estimates. Moreover, the Schlegel et al. (1998) estimate of the reddening in this direction can be safely used as an additional constraint. On the other hand, the CMDs of Be 23 and King 8 are both sufficiently contaminated and affected by reddening that the RC position is a necessary constraint to derive their ages. Relaxing the assumption on the RC position greatly expands the range of possible ages, and the only derivable result is that both clusters are certainly younger than 2 Gyr. Still, we believe that, although admittedly few, the stars in the CMD RC region are most likely cluster members and can therefore be used in the analysis. A definitive confirmation clearly needs proper motion or studies of RV.

With the present study we may have reached the limit of what is possible to derive simply with photometric data. Next step will be provided by *Gaia*, the satellite due to fly in about two years, which will produce photometry for about 10^9 Galactic objects, and most importantly, parallaxes and proper motions of unprecedented precision. The expected performances of *Gaia* will permit us to obtain individual distances of RC stars better than 10 per cent up

[6] Assuming a Galactocentric distance of the Sun of 8 kpc.

Downloaded from http://mnras.oxfordjournals.org/ at UniversitÃ di Pisa on October 13, 2016

to 8–10 kpc from the Sun, i.e. including almost the entire family of known OCs. The precision on proper motions will be even better (the estimated error on proper motions is about half the one on parallax), so that membership for a large fraction of stars will be available also for distant clusters. This will be important especially in cases like Be 31, where the separation in RV between field and cluster stars is very small (see Section 1).

ACKNOWLEDGMENTS

We are grateful to the referee, Bruce Twarog, for his constructive and helpful comments, that allowed us to significantly improve our paper. We thank Paolo Montegriffo for his software. This paper has made use of the WEBDA data base, operated at the Institute for Astronomy of the University of Vienna, of the SIMBAD data base, operated at CDS, Strasbourg, France, and of NASA's Astrophysics Data System. We are grateful to the LBC team for the pre-reduction procedures.

REFERENCES

Ahumada J. A., Lapasset E., 2007, A&A, 463, 789
Andreuzzi G., Bragaglia A., Tosi M., Marconi G., 2011, MNRAS, 412, 1265
Ann H. B. et al., 2002, AJ, 123, 905
Beccari G., Ferraro F. R., Possenti A., Valenti E., Origlia L., Rood R. T., 2006, AJ, 131, 2551
Bellazzini M., Fusi Pecci F., Messineo M., Monaco L., Rood R. T., 2002, AJ, 123, 1509
Bragaglia A., Tosi M., 2006, AJ, 131, 1544
Bressan A., Fagotto F., Bertelli G., Chiosi C., 1993, A&AS, 100, 647
Castellani V., Degl'Innocenti S., Girardi L., Marconi M., Prada Moroni P. G., Weiss A., 2000, A&A, 354, 150
Castellani V., Degl'Innocenti S., Marconi M., Prada Moroni P. G., Sestito P., 2003, A&A, 404, 645
Christian C. A., 1981, ApJ, 246, 827
Christian C. A., 1984, ApJ, 286, 552
Cignoni M., Tosi M., Bragaglia A., Kalirai J. S., Davis D. S., 2008, MNRAS, 386, 2235
Dias W. S., Lépine J. R. D., Alessi B. S., 2002a, A&A, 388, 168
Dias W. S., Alessi B. S., Moitinho A., Lépine J. R. D., 2002b, A&A, 389, 871
Dominguez I., Chieffi A., Limongi M., Straniero O., 1999, ApJ, 524, 226
Fagotto F., Bressan A., Bertelli G., Chiosi C., 1994, A&AS, 105, 29
Freeman K., Bland-Hawthorn J., 2002, ARA&A, 40, 487
Friel E. D., 1995, ARA&A, 33, 381
Friel E. D., Janes K. A., 1993, A&A, 267, 75
Friel E. D., Janes K. A., Tavarez M., Scott J., Katsanis R., Lotz J., Hong L., Miller N., 2002, AJ, 124, 2693
Friel E. D., Jacobson H. R., Pilachowski C. A., 2010, AJ, 139, 1942
Guetter H. H., 1993, AJ, 106, 220
Hasegawa T., Malasan H. L., Kawakita H., Obayashi H., Kurabayashi T., Nakai T., Hyakkai M., Arimoto N., 2004, PASJ, 56, 295
Hurley J., Tout C. A., 1998, MNRAS, 300, 977
King I. R., 1966, AJ, 71, 64
Koposov S. E., Glushkova E. V., Zolotukhin I. Y., 2008, A&A, 486, 771
Landolt A. U., 1992, AJ, 104, 340
Lanzoni B. et al., 2010, ApJ, 717, 653
Martin N. F., Ibata R. A., Bellazzini M., Irwin M. J., Lewis G. F., Dehnen W., 2004, MNRAS, 348, 12
Momany Y., Zaggia S., Gilmore G., Piotto G., Carraro G., Bedin L. R., de Angeli F., 2006, A&A, 451, 515
Panagia N., Tosi M., 1981, A&A, 96, 306
Phelps R. L., Janes K. A., Montgomery K. A., 1994, AJ, 107, 1079
Schlegel D. J., Finkbeiner D. P., Davis M., 1998, ApJ, 500, 525
Sigurdsson S., Phinney E. S., 1995, APJS, 99, 609
Sollima A., Carballo-Bello J. A., Beccari G., Ferraro F. R., Pecci F. F., Lanzoni B., 2010, MNRAS, 401, 577
Stetson P. B., 1987, PASP, 99, 191
Stetson P. B., 1994, PASP, 106, 250
Svolopoulos S. N., 1965, Z. Astrophys., 61, 97
Tosi M., Bragaglia A., Cignoni M., 2007, MNRAS, 378, 730
Twarog B. A., Anthony-Twarog B. J., 1989, AJ, 97, 759
Twarog B. A., Ashman K. M., Anthony-Twarog B. J., 1997, AJ, 114, 2556
Ventura P., Zeppieri A., Mazzitelli I., D'Antona F., 1998, A&A, 334, 953
Yong D., Carney B. W., Teixera de Almeida M. L., 2005, AJ, 130, 597

This paper has been typeset from a TEX/LATEX file prepared by the author.

Downloaded from http://mnras.oxfordjournals.org/ at UniversitÃ di Pisa on October 13, 2016